FEBS Letters

FEBS PRESS science publishing by scientists

# NADH/NAD$^+$ binding and linked tetrameric assembly of the oncogenic transcription factors CtBP1 and CtBP2

Heidi Erlandsen[1], Anne M. Jecrois[2], Jeffry C. Nichols[2,3], James L. Cole[4] and William E. Royer Jr[2]

1 Center for Open Research Resources & Equipment, University of Connecticut, Storrs, CT, USA
2 Department of Biochemistry and Molecular Biotechnology, UMass Chan Medical School, Worcester, MA, USA
3 Chemistry Department, Worcester State University, MA, USA
4 Department of Molecular and Cell Biology, Department of Chemistry, University of Connecticut, CT, USA

**Correspondence**
W. E. Royer Jr, Department of Biochemistry and Molecular Biotechnology, UMass Chan Medical School, 364 Plantation Street, Worcester, MA 01605, USA
Tel: +1 508-856-6912
E-mail: william.royer@umassmed.edu
J. L. Cole, Department of Molecular and Cell Biology, Department of Chemistry, University of Connecticut, 91 North Eagleville Road, U-3125, Storrs, CT 06269, USA
Tel +1 860 486-4333
E-mail: james.cole@uconn.edu

(Received 6 October 2021, revised 14 December 2021, accepted 22 December 2021)

doi:10.1002/1873-3468.14276

Edited by Michael Bubb

**The activation of oncogenic C-terminal binding Protein (CtBP) transcriptional activity is coupled with NAD(H) binding and homo-oligomeric assembly, although the level of CtBP assembly and nucleotide binding affinity continues to be debated. Here, we apply biophysical techniques to address these fundamental issues for CtBP1 and CtBP2. Our ultracentrifugation results unambiguously demonstrate that CtBP assembles into tetramers in the presence of saturating NAD$^+$ or NADH with tetramer to dimer dissociation constants about 100 nM. Isothermal titration calorimetry measurements of NAD(H) binding to CtBP show dissociation constants between 30 and 500 nM, depending on the nucleotide and paralog. Given cellular levels of NAD$^+$, CtBP is likely to be fully saturated with NAD under physiological concentrations suggesting that CtBP is unable to act as a sensor for NADH levels.**

**Keywords:** cancer target; cotranscriptional factor; NAD(H); protein assembly

C-terminal binding proteins (CtBP1 and CtBP2) are paralogs that critically modulate cell fate through their cotranscriptional activity. CtBP1 was initially identified through its binding of the C-terminal region of adenovirus E1A oncoprotein and resultant modulation of E1A transformation capability [1,2]. Binding of CtBP to transcription factors influences numerous cellular processes through recruitment of chromatin remodelling enzymes such as histone methyl transferases, demethylases and deacetylases to targeted promoters [3–5].

Extensive evidence implicates the cotranscriptional function of both CtBP paralogs in cancer. CtBP is a global repressor of apoptotic pathways and the epithelial phenotype [3] through the repression of genes such as cell cycle inhibitors, tumour suppressive proapoptotic factors (*Bik*, *Noxa*) and cytoskeletal/cell adhesion molecules (*keratin-8*, *E-cadherin*) [4,6]. In addition to its role as a corepressor, CtBP also facilitates activation of cell growth and metastasis-related genes (*Tiam1*, *MDR1*, certain Wnt target genes) that promote the epithelial-to-mesenchymal transition (EMT) [7–10]. Consistent with its transcriptional activity, CtBP is found to be upregulated in cancer tissues including colorectal cancer [11], melanoma [12], metastatic prostate cancer [13], oesophageal squamous cell carcinoma [14], ovarian cancer [15] and breast cancer [16,17]. Moreover, high tumour expression of CtBP is correlated with increased mortality in breast cancer

**Abbreviations**
CtBP, C-terminal binding protein; NAD, nicotinamide adenine dinucleotide.

[18], ovarian cancer [15], gastric carcinoma [19] and hepatocellular carcinoma [20]. Mouse models provide further evidence of a strong role for CtBP in cancer progression by showing that decreasing CtBP protein levels with $CtBP2^{+/-}$ heterozygosity result in a significant decrease in mortality for colon cancer ($APC^{min/+}$) [21] and pancreatic adenocarcinoma (CKP) models [22].

Oligomerization of transcriptional factors is an important paradigm for the regulation of gene expression [23,24]. Although NAD(H) binding to CtBP has been linked to oligomerization and transcriptional activity for nearly two decades [25,26], the level of assembly and the relative affinity of NADH vs $NAD^+$ are key issues without consensus at present. Numerous reports have suggested that NAD(H) triggers activation through assembly of CtBP monomers into dimers [27–30], but others have shown evidence that NAD(H) triggers assembly of dimers into tetramers [31–33]. Additionally, published data of the affinity of NADH and $NAD^+$ binding to CtBP have led to conflicting conclusions [33–35]. In particular, studies suggesting a 100-fold increased affinity of NADH over that of $NAD^+$ [34,35] led to the appealing hypothesis that CtBP acts as a sensor of the cellular metabolic state, which continues to be a highly cited conclusion.

Here, we investigate the NAD(H)-linked assembly of CtBP through analytical ultracentrifugation and isothermal titration calorimetry (ITC). Despite earlier interpretations of sedimentation velocity (SV) data as deriving from a monomer to dimer assembly [36], we definitively show using both SV and sedimentation equilibrium (SE) that the NAD(H) bound forms of both CtBP1 and CtBP2 are predominantly tetrameric in solution at micromolar concentrations. This tetrameric assembly is fairly stable – our SV experiments show that the tetramer to dimer dissociation constants for CtBP1 and CtBP2 in the presence of saturating NADH or $NAD^+$ are around 100 nM. Our ITC data indicate that CtBP binds to $NAD^+$ and NADH with dissociation constants between ~30 and ~500 nM, depending on the nucleotide and paralog. These results suggest that under normal cellular conditions, with $NAD^+$ levels > 40 μM [37–39], CtBP will be nearly fully saturated with NAD and unable to act as a sensor for NADH levels.

## Experimental procedures

### Expression and purification of CtBP1 and CtBP2

CtBP1 (28–440) and CtBP2 (31–445) were expressed and purified following the protocols of earlier studies [31,40,41]. The final step of purification was an FPLC size exclusion column (Highload■ 16/60 Superdex■ 200 preparation grade) carried out at 4 °C in buffer (50 mM Tris : HCl pH 7.7, 300 mM NaCl, 5 mM EDTA, 2 mM DTT) that was supplemented with either 50 μM $NAD^+$, 5 mM AMP or no nucleotide, depending on the experiment. Purified protein was buffer exchanged using a PD-10 Desalting Column (MilliporeSigma, Burlington, MA, USA). For the standard analytical ultracentrifugation experiments, this buffer was 50 mM HEPES pH 7.5, 300 mM NaCl, 5 mM EDTA, 2 mM TCEP with, or without varying amounts of $NAD^+$ or NADH. For lower concentration SV measurements using the peptide backbone absorption, a buffer of 10 mM HEPES (pH 7.5), 300 mM NaCl, 5 μM NAD(H), 0.1 mM EDTA and 0.4 mM TCEP was used to minimize the buffer absorbance at 230 nm. In the case of ultracentrifugation and calorimetry experiments requiring NAD(H)-free protein, we followed our earlier approach [41] of using, as the final step in purification, a size exclusion chromatography run in the presence of 5 mM AMP to remove NAD(H). X-ray crystal structures confirmed that this procedure resulted in the complete removal of NAD(H) for CtBP1 [41] and size exclusion chromatography and light scattering indicate successful removal from CtBP2. AMP was then removed with a PD-10 desalting column.

### Analytical ultracentrifugation

Partial-specific volumes and solvent densities and viscosities were determined using SEDNTERP [42]. SV analysis was performed using two-channel aluminium-Epon double-sector centrepieces and quartz windows. Absorbance data were collected in a Beckman-Coulter Optima analytical ultracentrifuge operating at 35 000 r.p.m. and 20 °C. $c(s)$ distributions were calculated using SEDFIT [43].

Dissociation constants for the dimer–tetramer equilibria of nucleotide bound forms of CtBP1 and CtBP2 were obtained by SV analysis at 230 nm to enhance sensitivity. The weight-average sedimentation coefficients ($s_w$) were obtained by integration of $c(s)$ distributions, and the data were fit to the following equation

$$S_w = \frac{S_D[D] + 2S_T[D]}{[D] + 2[D]} \quad (1)$$

where $s_D$ and $s_T$ are the sedimentation coefficients of dimer and tetramer, respectively, and [D] and [T] are the molar concentrations of dimer and tetramer, respectively. The dimer concentration is given by

$$[\mathrm{D}] = \frac{-1 + \sqrt{1 + 8[P]_t/K_d}}{4/K_d} \quad (2)$$

where $[P]_t$ is the total concentration of protein in dimer equivalents. For comparison to the weight-average analysis, the SV data were also globally fit to dimer–tetramer equilibrium model using SEDANAL [44]. At the lowest accessible protein concentration of 0.3 μM, both CtBP1 and CtBP2 are predominantly tetrameric in the presence of bound nucleotide and it was not feasible to fit for $s_D$. For CtBP2, this parameter was taken as the sedimentation coefficient of the apoprotein dimer (4.02 S), and for CtBP1, it was taken as 3.96 S by assuming equal frictional ratios for the two proteins. For SV analysis of nucleotide-free CtBP1, it was necessary to account for the presence of monomer in the weight-average and global fits. Here, the sedimentation coefficient of the monomer was taken as 2.49 S assuming an equal frictional ratio for the monomer and dimer. The $s_w$ data were fit using numerical solutions to the monomer–dimer–tetramer equilibria.

Sedimentation equilibrium analysis was performed using six-channel aluminium-Epon double-sector centrepieces and quartz windows. Absorbance data at 280 nm were collected in a Beckman-Coulter XL-I analytical ultracentrifuge at 20 °C and 9500 and 11 500 r.p.m. Data were globally fit to a single ideal species model using HeteroAnalysis [45].

### Isothermal titration calorimetry

Isothermal titration calorimetry (ITC) analysis of $NAD^+$/NADH binding to nucleotide-free CtBP1 and CtBP2 used protein prepared as described above. CtBP1 and CtBP2 appear significantly less stable in the absence of bound nucleotide. For this reason, ITC experiments were carried out immediately upon elution from the PD-10 column, equilibrated with 50 mM HEPES pH 7.5, 300 mM NaCl, 5 mM EDTA, 2 mM TCEP, with final protein concentration at 10–50 μM. (As our SV data demonstrated significant dissociation of nucleotide-free CtBP1 into dimers, particularly below a protein concentration of around 10 μM, we attempted ITC binding experiments at protein concentrations below 10 μM to explore changes in apparent binding affinity as the proportion of dimers increase. Unfortunately, these lower concentration experiments did not provide reproducible results.)

Isothermal titration calorimetry measurements were performed on a Microcal ITC200 System (GE, Boston, MA, USA). For the final runs with CtBP1, 20 injections, 2 μL each, of either 0.2 mM NADH or 0.5 mM $NAD^+$ were used for each measurement. For CtBP2, 20 injections, 1.5–2 μL each, of either 0.2mM NADH or 0.4 mM $NAD^+$ were used for each measurement. Data were fit in Origin software to a single binding site model. Heats of ligand dilution were obtained following binding saturation using the later injections and subtracted for each binding experiment.

## Results

### Assembly state of CtBP1 and CtBP2

Previous SV experiments on truncated CtBP2 (31–364), in which the first 30 residues and the critical last 91 residues are missing, identified a predominant species with a sedimentation coefficient of 6.0–6.7 S [36]. This species was assumed to be dimeric. An $s = 4.3$ S species, enhanced in the presence of mutants or an inhibitor, was assigned as monomer. As our light scattering data showing a predominantly tetrameric form for truncated CtBP2 (31–364; as well as longer forms of CtBP1 and CtBP2) in the presence of NADH or $NAD^+$ [31] was inconsistent with that interpretation, we have carried out SV and SE analyses to resolve this discrepancy.

Figure 1A,B shows SV $c(s)$ distributions [43] for CtBP1 (28–440) and CtBP2 (31–445), respectively, as purified in the absence of added nucleotide. Both proteins contain a dominant feature near 6 S. CtBP1 contains several peaks at lower $s$, and CtBP2 contains a 4.1 S peak. For both proteins, as the concentration is decreased from 40 to 2 μM, the peak near 6 S shifts slightly to the left, indicating that it represents a reaction boundary associated with a rapidly reversible self-association. Concentration-dependent behaviour of the 3–5 S features for CtBP1 is not as clear, but these features also appear to shift to the left with decreasing concentration. For CtBP2, the peak near 4.1 S does not shift with concentration. Discrete fits to the data indicate that the fraction of material sedimenting at 4.1 S increases only slightly from ~ 0.3 to ~ 0.5 as the concentration is decreased from 40 to 2 μM. These data indicate that the 4.1 S peak corresponds to a discrete species that undergoes weak self-association.

Figure 1C,D show a sedimentation velocity analysis of the effects of NADH binding on CtBP1 and CtBP2. Data were collected at 280 and 340 nm to selectively monitor the protein and NADH components, respectively. For both proteins, the lower $s$ peaks disappear upon addition of NADH, producing a single peak near 6 S. The 340 nm data demonstrate that NADH cosediments with CtBP1 and CtBP2 near 6 S. Based on these results, we assign the lower $s$ peaks to

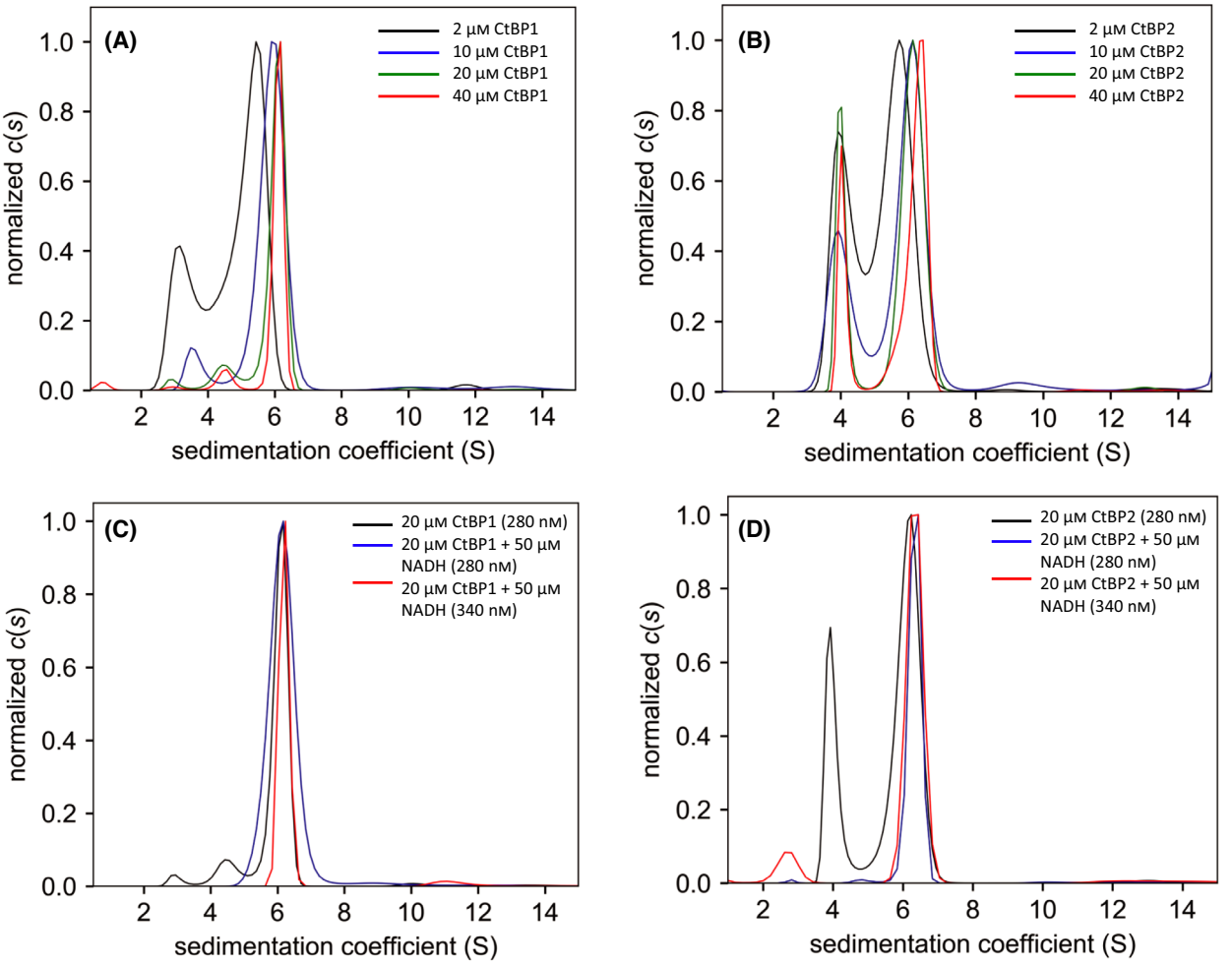


**Fig. 1.** Sedimentation velocity analysis of CtBP1 and CtBP2 self-association. (A) *c*(*s*) distribution of CtBP1 as purified [no added NAD(H); at 2, 10, 20 and 40 μM (monomer equivalents)]; (B) *c*(*s*) distributions of CtBP2 as purified (no added NAD(H); at 2, 10, 20 and 40 μM); C) 20 μM CtBP1 as purified (no added NAD(H)) compared to CtBP1 with 50 μM NADH at 280 and 340 nm wavelength (340 nm/NADH signal is red) and (D) 20 μM CtBP2 as purified (no added NAD(H)) compared to CtBP2 with 50 μM NADH at 280 and 340 nm wavelength (340 nm/NADH signal is red). All of the distributions are normalized by maximum peak height.

apoprotein and the 6 S peaks to the NADH complexes.

The presence of the 6 S peak in the absence of added nucleotide suggests that an appreciable fraction of both CtBP1 and CtBP2 is nucleotide bound. However, the 340 nm absorbance of both proteins, as purified, is < 10% of what would be expected if the bound nucleotide were NADH (data not shown). NADH has absorption peaks at 340 and 260 nm, whereas $NAD^+$ only absorbs at 260 nm. Thus, the low 340 nm absorbance may indicate that both proteins contain bound $NAD^+$ or another adenine nucleotide species capable of inducing self-association of CtBPs.

Owing to the heterogeneity and the reversible self-association in both paralogs, it was not feasible to fit the SV data to obtain reliable molecular masses and we turned to SE measurements. Data were collected over a concentration range of 3–13 μM and two rotor speeds in the presence of 50 μM NAD(H). Within error, the apparent molecular masses of the individual channels remain constant over this concentration range, indicating that the dissociation of the tetramer is negligible and the data were globally fit to a model of a single ideal species. Figure 2 shows a fit obtained with CtBP2. The data fit well to this model with the inset showing randomly distributed residuals. The deduced molecular mass of 192.1 kDa (Table 1) corresponds to the tetramer (predicted mass of 191.0 kDa). Similarly, the best-fit molecular masses of CtBP2 in the presence of $NAD^+$ or CtBP1 with either nucleotide

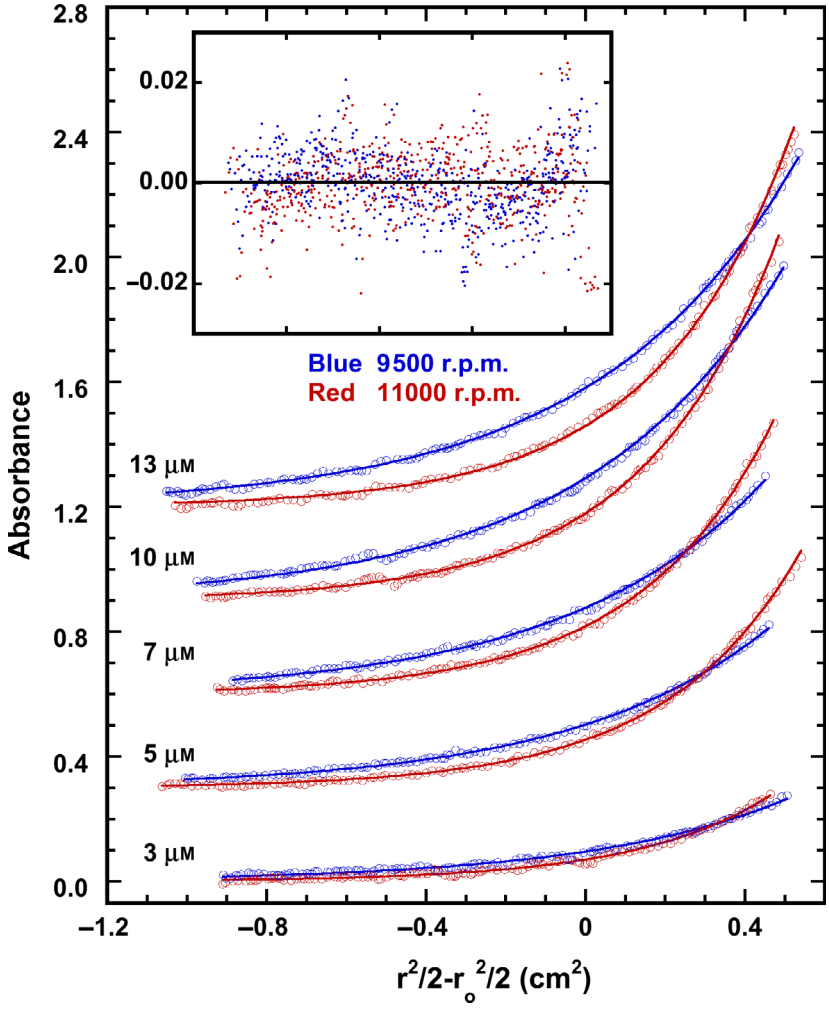


**Fig. 2.** Sedimentation equilibrium analysis of CtBP2 self-association in the presence of 50 μM NADH. Data (open circles) were collected at five protein concentrations ranging from 3 to 13 μM with 50 μM NADH at two rotor speeds: 9500 r.p.m. (blue) and 11 000 r.p.m. (red) at a wavelength of 280 nm. For clarity, the data are vertically offset. The solid lines correspond to a global fit of the data to a single ideal species model. The best-fit molecular mass is 192.1 kDa with an RMS deviation of 0.00642 OD. The inset shows an overlay of the fit residuals.

**Table 1.** Sedimentation equilibrium analysis of CtBP1 and CtBP2 in the presence of NADH or $NAD^+$.

| Protein: Ligand | Molecular mass (kDa)[a] | RMS[b] |
|---|---|---|
| CtBP1: $NAD^+$ | 176.3 (171.5, 181.2) | 0.00435 |
| CtBP1: NADH | 176.1 (170.7, 181.6) | 0.00530 |
| CtBP2: $NAD^+$ | 184.5 (175.9, 193.3) | 0.01172 |
| CtBP2: NADH | 192.1 (186.4, 197.9) | 0.00642 |

[a]The range in parentheses corresponds to the 95% confidence intervals.; [b]Root mean square deviation of the fit in absorbance units.

also correspond to tetramer. These results agree with our previous light scattering analysis of CtBP1 and CtBP2 [31] and indicate that the SV feature near 6 S populated in the presence of nucleotide is associated with the tetramer rather than dimer, as has been previously suggested [36]. We then assign the 4.1 S feature to dimer. Based on these assignments, the frictional ratios of both the tetramer and the dimer are about 1.6. This high value is consistent with the presence of substantial disordered regions. Unlike earlier SV experiments [36], our CtBP1 and CtBP2 constructs incorporate the full C terminus, including ~ 90 C-terminal residues that have been shown to be intrinsically unstructured in rat CtBP [46] and show no ordered structure in the cryoEM structure of human CtBP2 [32].

## Dissociation of CtBP tetramers

In the presence of either NADH or $NAD^+$, both CtBP1 and CtBP2 are predominantly tetrameric at concentrations of 2 μM and above, but our SV results indicate some dissociation as the concentration is lowered. Because the protein aromatic side chain absorbance at 280 nm is too weak to characterize the dimer–tetramer equilibrium, we took advantage of the greater peptide backbone absorption at 230 nm. Due to buffer absorption at this wavelength, we reduced

the concentrations of several components while maintaining the same pH and NaCl concentration [10 mM HEPES (pH 7.5), 300 mM NaCl, 5 μM NAD(H), 0.1 mM EDTA and 0.4 mM TCEP]. Under these conditions, reasonable SV data were obtained down to protein concentrations as low as 300 nM. The weight-average sedimentation coefficients ($s_w$) were obtained from SV titrations from 300 nM to 5 μM, and the resulting isotherms are displayed in Fig. 3. For both CtBP1 and CtBP2, $s_w$ increases from ~ 5.4 to 6.1 S over this concentration range. These data were fit to dimer–tetramer equilibrium models to obtain $K_d$ values, which are displayed in Table 2.

Even with the enhanced sensitivity at 230 nm, it was not possible to reduce the concentration low enough to allow us to fit for the sedimentation coefficient of the dimer. As described in Materials and Methods, the values for the dimer sedimentation coefficients were taken from the apoprotein dimers. The fitted $K_d$s for CtBP1 and CtBP2 in $NAD^+$ or NADH are quite similar, ranging from 76 to 94 nM. The tetramer sedimentation coefficients are also close, ranging from 6.4 to 6.6 S. To confirm this analysis, we also globally analysed SV difference curves obtained at multiple concentrations using SEDANAL [44], again fixing the sedimentation coefficients of the dimer. An example fit for CtBP2 + $NAD^+$ is shown in Fig. S1. As indicated in Table 1, the parameters obtained by the two approaches agree fairly well.

Sedimentation velocity experiments were also performed with nucleotide-free CtBP, prepared with size exclusion in the presence of 5 mM AMP [41], as discussed in the Experimental procedures section. As

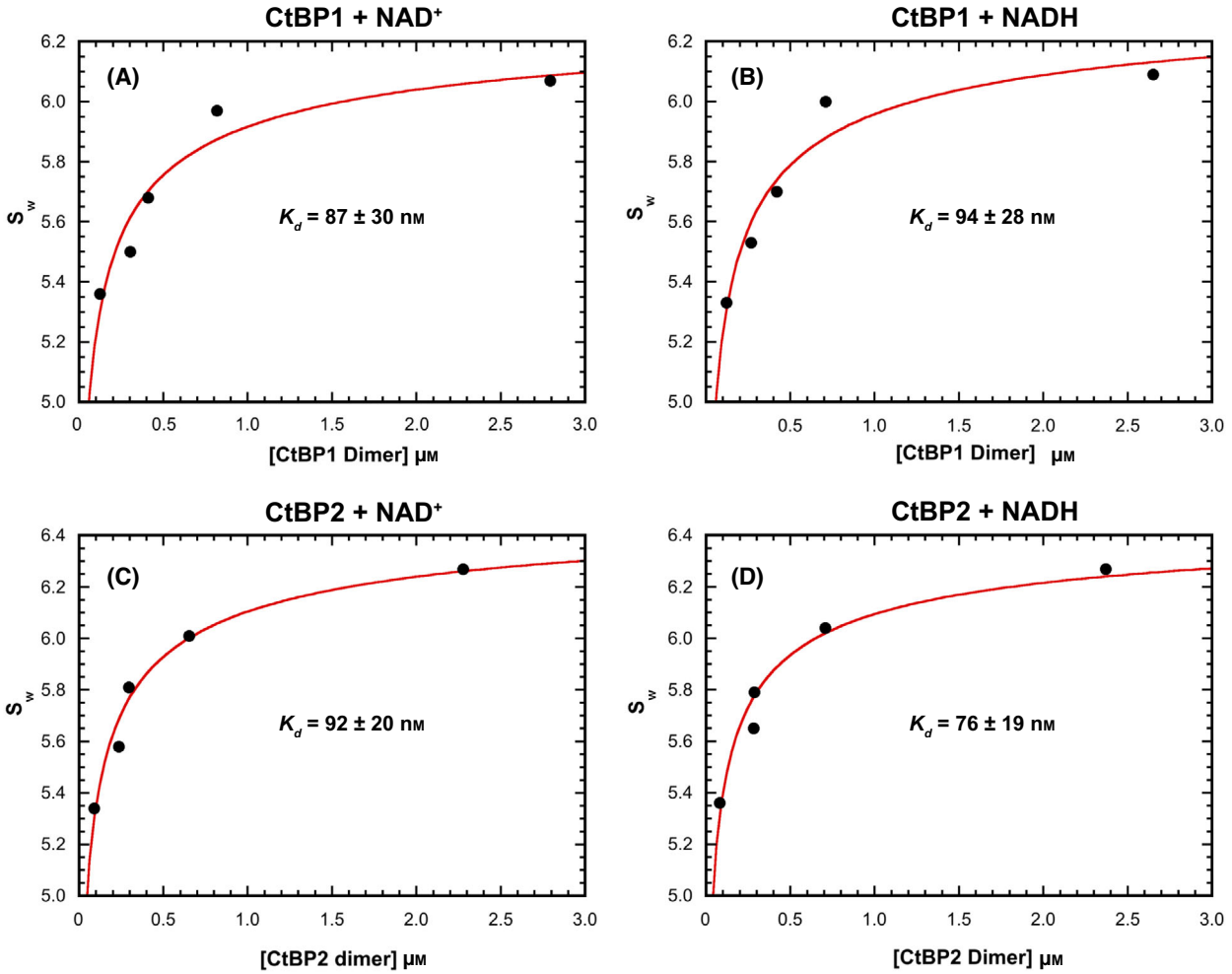


**Fig. 3.** Determination of CtBP1 and CtBP2 dissociation constants: weight-average sedimentation coefficient analysis. (A) CtBP1 + $NAD^+$; (B) CtBP1 + NADH; (C) CtBP2 + $NAD^+$; (D) CtBP2 + NADH. Dissociation constants were obtained by fitting isotherms of weight-average sedimentation coefficients ($s_w$) to a dimer-tetramer equilibrium model. The values of $s_{dimer}$ were fixed at 3.96 S (CtBP1) and 4.02 S (CtBP2), and $s_{tetramer}$ and $K_d$ were treated as adjustable parameters.

**Table 2.** Analysis of the dimer–tetramer equilibria for CtBP1 and CtBP2 in the presence of NADH or $NAD^+$.

| | Global[a] | | | Weight average[b] | |
|---|---|---|---|---|---|
| Protein: Ligand | $s_{Tetramer}$ | $K_d$ (nM)[c] | RMSD[d] | $s_{Tetramer}$ | $K_d$ (nM) |
| CtBP1: $NAD^+$ | 6.48 | 140.0 (121.5, 161.8) | 0.0147 | 6.37 | 87 ± 30 |
| CtBP1: NADH | 6.49 | 94.2 (81.8, 171.8) | 0.0190 | 6.44 | 94 ± 28 |
| CtBP2: $NAD^+$ | 6.64 | 103.1 (78.2, 132.6) | 0.0119 | 6.60 | 92 ± 20 |
| CtBP2: NADH | 6.70 | 94.7 (80.9, 109.9) | 0.0156 | 6.54 | 76 ± 19 |

[a]Parameters were obtained by global analysis of sedimentation velocity data difference curves using SEDANAL [44].; [b]Parameters were obtained by fitting the isotherm of weight-average sedimentation coefficients as described in the Materials and Methods section.; [c]The range in parentheses corresponds to the 95% confidence intervals.; [d]Root mean square deviation of the fit in absorbance units.

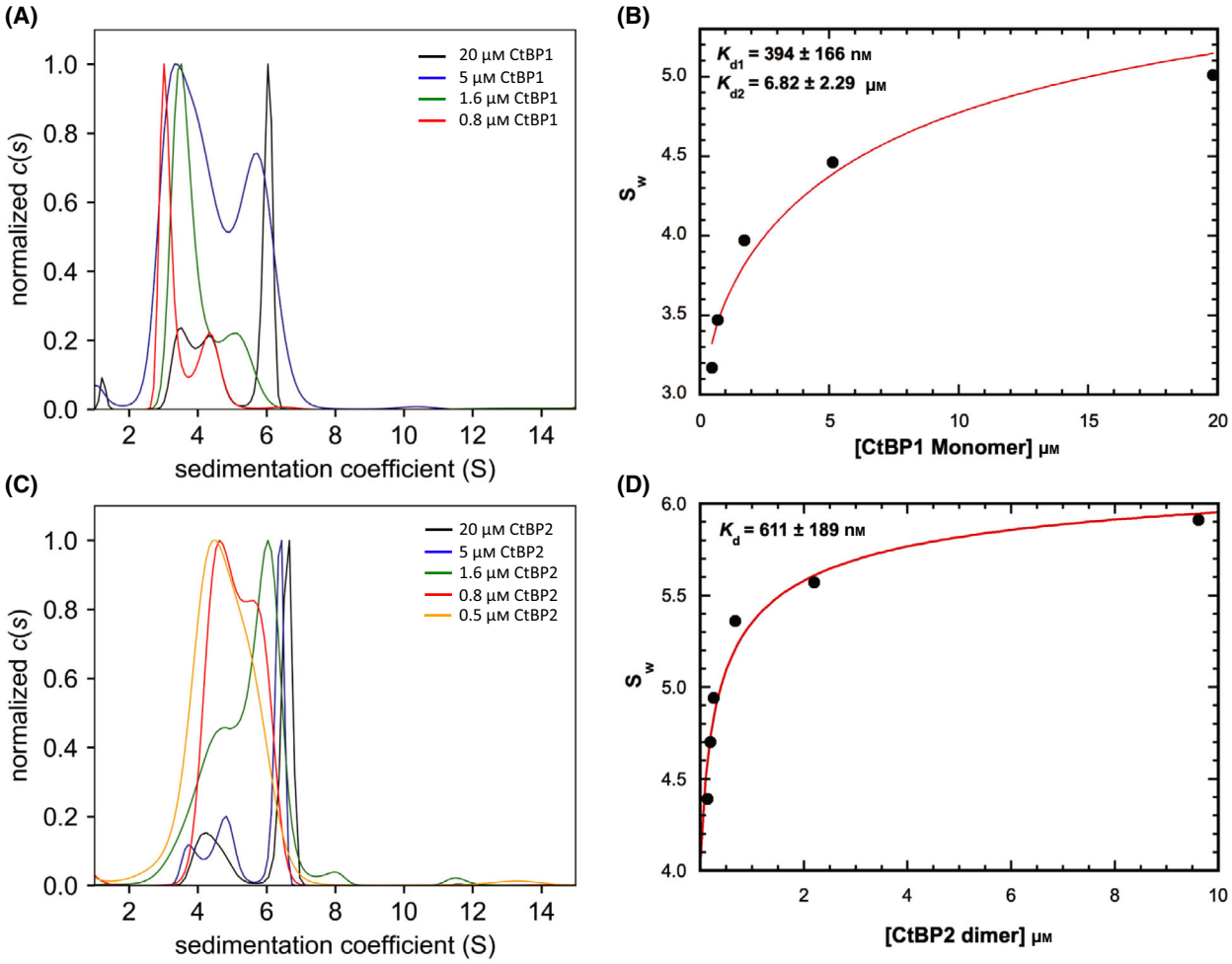


**Fig. 4.** Sedimentation velocity analysis of nucleotide-free CtB1 and CtBP2. (A) *c*(*s*) distribution of CtBP1 (at 0.8, 1.6, 5 and 20 μM); (B) weight-average determination of CtBP1 dissociation constants; (C) *c*(*s*) distribution of CtBP2 (at 0.5, 0.8, 1.6, 5 and 20 μM); (D) weight-average determination of CtBP2 dissociation constants. For CtBP1, the dissociation constants were obtained by fitting to a monomer–dimer–tetramer equilibrium model, and for CtBP2, a dimer–tetramer model was employed. $K_{d1}$ refers to the monomer–dimer dissociation constant, and $K_{d2}$ refers to the dimer–tetramer dissociation constant.

shown in Fig. 4, the tetrameric forms are notably less stable in the absence of $NAD^+$, as would be expected. For CtBP1, the *c*(*s*) distributions contain a predominant 6 S feature (tetramer) at the highest concentration (20 μM) which shifts to the left as the concentration is reduced. The distributions at the lowest

**Table 3.** Analysis of the monomer–dimer–tetramer equilibria for CtBP1 and CtBP2 in the absence of bound nucleotide.

| | Global[a] | | | Weight average[b] | |
|---|---|---|---|---|---|
| Protein | $K_{d1}$ (nM)[c] | $K_{d2}$ (nM)[d] | RMSD[e] | $K_{d1}$ (nM) | $K_{d2}$ (nM) |
| CtBP1 | 968 ( 760, 1220) | 3320 (2880, 3810) | 0.0244 | 394 ± 166 | 6820 ± 2290 |
| CtBP2 | – | 967 (909, 1030) | 0.0248 | – | 611 ± 189 |

[a]Parameters were obtained by global analysis of sedimentation velocity data difference curves using SEDANAL [44].; [b]Parameters were obtained by fitting the isotherm of weight-average sedimentation coefficients as described in the Materials and Methods section.; [c]Monomer–dimer dissociation constant.; [d]Dimer–tetramer dissociation constant.; [e]Root mean square deviation of the fit in absorbance units

concentrations contain features below 4 S, indicating dissociation all the way to monomer. In contrast, CtBP2 dissociates from tetramer to dimer upon dilution. Accordingly, the CtBP1 and CtBP2 data were fit to monomer–dimer–tetramer and dimer–tetramer equilibrium models, respectively. The $K_d$ values obtained by weight-average (Fig. 4B,D) and global analyses agree reasonably well (Table 3). Including a monomer–dimer dissociation reaction in the analysis CtBP2 did not substantially improve the fit quality (RMSD = 0.0238) whereas fitting the CtBP1 data to a dimer–tetramer model resulted in substantially worse fit (RMSD = 0.0351). For CtBP1 and CtBP2, dissociation of the nucleotide-free tetramers to dimers is enhanced ~50- and ~8-fold, respectively, relative to their corresponding nucleotide bound forms. For CtBP1, dissociation of the dimer to monomer occurs at sub-micromolar concentrations.

## Binding of NADH and NAD$^+$ to CtBP

Removal of NADH from CtBP is known to be difficult [34], which may have contributed to the wide variations reported for estimates of NADH and NAD$^+$ affinity. Here, we have used high levels of AMP to remove NAD(H) as described previously [41]. Details are discussed in the Experimental procedures section.

Isothermal titration calorimetry experiments monitoring the binding of NAD$^+$ and NADH were performed with freshly prepared CtBP in the absence of any bound nucleotide. Although nucleotide-free CtBP is substantially less stable than the nucleotide bound form, we were able to obtain excellent ITC data for the binding of NAD$^+$ and NADH to CtBP1 at 23 °C. As shown in Fig. 5 and Table 4, these ITC experiments showed that CtBP1 (28–440) bound to NADH with a measured $K_d$ of 53 ± 14 nM, whereas the binding to NAD$^+$ was about 9-fold weaker with a $K_d$ of 450 ± 43 nM. CtBP2 appears to be somewhat less stable than CtBP1 in the absence of bound nucleotide, but binds NAD$^+$ substantially more tightly than does CtBP1. For CtBP2 (31–445), NADH bound with a measured $K_d$ of 31 ± 6 nM, whereas the binding to NAD$^+$ was nearly two-fold weaker with a $K_d$ of 51 ± 15 nM (Fig. 5 and Table 4). Given the SV data (Fig. 4, Table 3) showing that the CtBP2 tetramer is

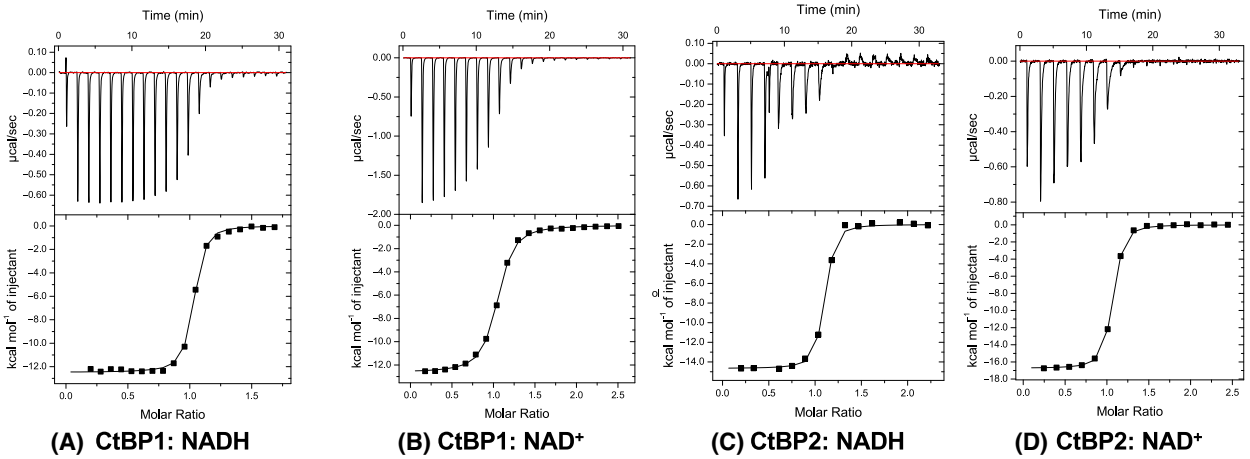


**Fig. 5.** Example ITC measurements of NADH and NAD$^+$ binding to CtBP1 and CtBP2 at 23 °C. (A) NADH binding to CtBP1 with 2 µL aliquots of 0.2 mM NADH, (B) NAD$^+$ binding to CtBP1 at with 2 µL aliquots of 0.5 mM NAD$^+$, (C) NADH binding to CtBP2 with 2 µL aliquots of 0.2 mM NADH, (D) NAD$^+$ binding to CtBP2 with 1.5 µL aliquots of 0.4 mM NAD$^+$. Full ITC results are provided in Table 4.

**Table 4.** Thermodynamic parameters for NAD(H) binding to CtBP derived from ITC experiments at 23 °C. (Reported values based on three replicates for each condition).

| Protein: Ligand | $K_d$ (nM) | $\Delta G$ (kcal·mol$^{-1}$) | $\Delta H$ (kcal·mol$^{-1}$) | $T\Delta S$ (kcal·mol$^{-1}$) |
|---|---|---|---|---|
| CtBP1-NADH | 53 ± 14 | −9.8 ± 0.1 | −12.6 ± 0.2 | −2.8 ± 0.4 |
| CtBP1-NAD$^+$ | 450 ± 43 | −8.6 ± 0.05 | −12.9 ± 0.3 | −4.3 ± 0.3 |
| CtBP2-NADH[a] | 31 ± 7 | −10.2 ± 0.1 | −15.1 ± 0.4 | −4.9 ± 0.4 |
| CtBP2-NAD$^+$ | 51 ± 15 | −9.9 ± 0.1 | −16.5 ± 0.4 | −6.6 ± 0.5 |

[a]For the CtBP2-NADH ITC experiments, all three replicates were from a single protein prep. For all others, the three replicates included two different protein preps.

more stable than the CtBP1 tetramer, one possible source of the observed higher affinity for CtBP2 is a greater fraction of nucleotide-free CtBP2 tetramers. Analysis of the nucleotide-free SV data suggests that ~ 90% of the CtBP2 is tetrameric and ~ 60% of CtBP1 is tetrameric at 40 μM (monomer equivalents) Unfortunately, ITC experiments on CtBP1 below 10 μM to help estimate the NAD(H) affinity of dimers were unsuccessful. While our results support the hypothesis that NADH binds to CtBP more tightly than does NAD$^+$, it is by a much smaller factor than the 100-fold difference that had been suggested earlier [34].

## Discussion

The transcriptional coregulators CtBP1 and CtBP2 have been implicated in a broad range of cancers [12–22]. It has long been established that binding of NAD(H) induces oligomerization and transcriptional activation of CtBP [25,26]. However, there are conflicting hypotheses about the level of oligomerization [27–33] and the relative affinity of binding NADH vs NAD$^+$ [33–35]. These issues are key to understanding the basis for transcriptional activation of CtBP and also for guiding the design of inhibitors to disrupt transcriptional activity in cancer. The analytical biophysical experiments presented here were designed to address these two central issues.

Earlier SV experiments on C-terminal truncated CtBP2 [36] revealed a predominant population with $s$ = 6–6.7, which was interpreted as dimeric, even in the presence of NAD(H). However, recent data from a variety of experimental methods suggest that binding of NAD(H) to CtBP triggers assembly of dimers into tetramers [31–33]. To definitively determine the level of CtBP assembly in solution, we turned to analytical ultracentrifugation.

For both CtBP1 and CtBP2, purified in the absence of NAD(H), SV showed a predominant form at micromolar concentrations with a sedimentation coefficient of ~ 6, in agreement with earlier studies [36]. SE measurements unambiguously demonstrate that this form corresponds to tetramer (Fig. 2 and Table 1). CtBP2 contains a second form at 4.1 S that is assigned as dimer. The 4.1 S peak disappears upon addition of NADH, indicating that this peak corresponds to apoprotein. For both proteins, the tetrameric assembly is fairly stable in the presence of saturating NADH or NAD$^+$ with dimer dissociation constants of about 100 nM. In the absence of bound NAD(H), CtBP1 and CtBP2 tetramers are substantially weakened with dissociation constants approximately 50- to 8-fold higher, respectively (Table 3). Thus, nucleotide binding is thermodynamically linked to assembly of dimers into tetramers. Nucleotide-free CtBP1 further dissociates to monomer with $K_d$ ~ 1 μM.

Our analytical ultracentrifugation results provide a definitive proof that CtBP1 and CtBP2 assemble into tetramers in the presence of NAD(H), which is supported by other recent studies [31–33], despite a common assumption that NAD(H) triggers a monomer to dimer assembly. This work is, thus, complementary to our recent finding that mutants which interfere with dimer to tetramer assembly are transcriptionally defective for at least some oncogenic activity [32]. Moreover, our results suggest that sedimentation experiments could be an important assay to investigate the ability of various CtBP inhibitors [27,40,47,48] to directly disrupt transcriptionally dependent CtBP tetramer formation.

Our ITC results indicate that the $K_d$ for binding of NAD$^+$ to CtBP1 is approximately 450 nM with NADH binding approximately with 9-fold higher affinity. This result for NAD$^+$ binding is in alignment with equilibrium dialysis measurements reporting a $K_d$ of ~ 400 nM [33], and the 50 nM $K_d$ for NADH is close to the 66 nM $K_d$ reported using FRET experiments [34]. In contrast, our results indicate significantly tighter binding of NAD$^+$ than the 8–11 μM obtained by monitoring the loss of enhanced NADH fluorescence when bound to CtBP1 through competition with NAD$^+$ [34]. The nearly 100-fold greater protein concentration for our ITC experiments compared with the earlier fluorescence experiments could contribute to the reported NAD$^+$ affinity differences, since lower protein concentration would favour dissociation of tetramers to dimers and monomers with potentially lower nucleotide affinity. As ITC experiments require substantially higher protein concentrations than are likely in the cell, this is a potential advantage of the fluorescence approach. However, for the discrepancy between these two approaches to result from concentration

differences, lowered protein concentration would have to substantially alter the $NAD^+$ affinity but not the NADH affinity. The similar response of CtBP oligomerization to both $NAD^+$ and NADH shown here and earlier [31] would appear to argue against a strong concentration effect just for $NAD^+$. However, such a possibility cannot be completely discounted.

The earlier fluorescence studies [34] led to the appealing hypothesis that CtBP can act as a sensor for the metabolic state of a cell by sensing the concentration of NADH, as the cellular concentration of $NAD^+$ is much higher than NADH. This hypothesis requires that CtBP not be fully saturated by the $NAD^+$ present in the cell nucleus, since either $NAD^+$ or NADH is capable of triggering tetrameric assembly as shown here. Recent measurements using fluorescent biosensors suggest cytoplasmic levels of $NAD^+$ in the range of 40–80 μM in four mammalian cell lines with a level of $NAD^+$ of ~ 110 μM in the nucleus of U2OS cells [39], values that are consistent with earlier estimates in the range of 100–500 μM [37,38]. With cellular $NAD^+$ concentrations > 40 μM and our measured dissociation constants more than 100-fold lower, CtBP would be expected to be nearly fully saturated with $NAD^+$. Assuming that our ITC experiments at high protein concentration reasonably reflect the affinity of CtBP for NAD in the cellular context, these data argue against CtBP sensing the metabolic cellular state through changes in the concentration of NADH.

## Acknowledgements

We thank Dr. Celia Schiffer for discussions and acquisition of the Microcal ITC200 System. This work was supported by National Institutes of Health (NIH) grant R01 GM119014 to WER.

## Author contributions

HE, JLC and WER conceived and designed this study; HE, AMJ, JCN and WER performed the experiments; HE, JLC and WER analysed the results and wrote the manuscript.

## Data accessibility

Data that support the findings of this study are available on request from the corresponding authors.

## References

1 Boyd JM, Subramanian T, Schaeper U, La Regina M, Bayley S, Chinnadurai G. A region in the C-terminus of adenovirus 2/5 E1a protein is required for association with a cellular phosphoprotein and important for the negative modulation of T24-ras mediated transformation, tumorigenesis and metastasis. *EMBO J*. 1993;**12**:469–78.

2 Schaeper U, Boyd JM, Verma S, Uhlmann E, Subramanian T, Chinnadurai G. Molecular cloning and characterization of a cellular phosphoprotein that interacts with a conserved C-terminal domain of adenovirus E1A involved in negative modulation of oncogenic transformation. *Proc Natl Acad Sci USA*. 1995;**92**:10467–71.

3 Bergman LM, Blaydes JP. C-terminal binding proteins: emerging roles in cell survival and tumorigenesis. *Apoptosis*. 2006;**11**:879–88.

4 Chinnadurai G. The transcriptional corepressor CtBP: a foe of multiple tumor suppressors. *Cancer Res*. 2009;**69**:731–4.

5 Kuppuswamy M, Vijayalingam S, Zhao LJ, Zhou Y, Subramanian T, Ryerse J et al., Role of the PLDLS-binding cleft region of CtBP1 in recruitment of core and auxiliary components of the corepressor complex. *Mol Cell Biol*. 2008;**28**:269–81.

6 Grooteclaes M, Deveraux Q, Hildebrand J, Zhang Q, Goodman RH, Frisch SM. C-terminal-binding protein corepresses epithelial and proapoptotic gene expression programs. *Proc Natl Acad Sci USA*. 2003;**100**:4568–73.

7 Dcona MM, Morris BL, Ellis KC, Grossman SR. CtBP- an emerging oncogene and novel small molecule drug target: Advances in the understanding of its oncogenic action and identification of therapeutic inhibitors. *Cancer Biol Ther*. 2017;**18**:379–91.

8 Fang M, Li J, Blauwkamp T, Bhambhani C, Campbell N, Cadigan KM. C-terminal-binding protein directly activates and represses Wnt transcriptional targets in Drosophila. *EMBO J*. 2006;**25**:2735–45.

9 Jin W, Scotto KW, Hait WN, Yang JM. Involvement of CtBP1 in the transcriptional activation of the MDR1 gene in human multidrug resistant cancer cells. *Biochem Pharmacol*. 2007;**74**:851–9.

10 Paliwal S, Ho N, Parker D, Grossman SR. CtBP2 promotes human cancer cell migration by transcriptional activation of Tiam1. *Genes Cancer*. 2012;**3**:481–90.

11 Nadauld LD, Phelps R, Moore BC, Eisinger A, Sandoval IT, Chidester S et al., Adenomatous polyposis coli control of C-terminal binding protein-1 stability regulates expression of intestinal retinol dehydrogenases. *J Biol Chem*. 2006;**281**:37828–35.

12 Deng H, Liu J, Deng Y, Han G, Shellman YG, Robinson SE et al., CtBP1 is expressed in melanoma and represses the transcription of p16INK4a and Brca1. *J Invest Dermatol*. 2013;**133**:1294–301.

13 Wang R, Asangani IA, Chakravarthi BV, Ateeq B, Lonigro RJ, Cao Q et al., Role of transcriptional

corepressor CtBP1 in prostate cancer progression. *Neoplasia*. 2012;**14**:905–14.
14 Guan C, Shi H, Wang H, Zhang J, Ni W, Chen B et al., CtBP2 contributes to malignant development of human esophageal squamous cell carcinoma by regulation of p16INK4A. *J Cell Biochem*. 2013;**114**:1343–54.
15 Barroilhet L, Yang J, Hasselblatt K, Paranal RM, Ng SK, Rauh-Hain JA et al., C-terminal binding protein-2 regulates response of epithelial ovarian cancer cells to histone deacetylase inhibitors. *Oncogene*. 2013;**32**:3896–903.
16 Birts CN, Harding R, Soosaipillai G, Halder T, Azim-Araghi A, Darley M et al., Expression of CtBP family protein isoforms in breast cancer and their role in chemoresistance. *Biol Cell*. 2010;**103**:1–19.
17 Deng Y, Deng H, Liu J, Han G, Malkoski S, Liu B et al., Transcriptional down-regulation of Brca1 and E-cadherin by CtBP1 in breast cancer. *Mol Carcinog*. 2012;**51**:500–7.
18 Di LJ, Byun JS, Wong MM, Wakano C, Taylor T, Bilke S et al., Genome-wide profiles of CtBP link metabolism with genome stability and epithelial reprogramming in breast cancer. *Nat Commun*. 2013;**4**:1449.
19 Wang C, Wang M, Xing B, Chi Z, Wang H, Lie C et al., C-terminal of E1A binding protein 1 enhances the migration of gastric epithelial cells and has a clinicopathologic significance in human gastric carcinoma. *Onco Targets Ther*. 2019;**12**:5189–200.
20 Zheng X, Song T, Dou C, Jia Y, Liu Q. CtBP2 is an independent prognostic marker that promotes GLI1 induced epithelial-mesenchymal transition in hepatocellular carcinoma. *Oncotarget*. 2015;**6**:3752–69.
21 Sumner ET, Chawla AT, Cororaton AD, Koblinski JE, Kovi RC, Love IM et al., Transforming activity and therapeutic targeting of C-terminal-binding protein 2 in Apc-mutated neoplasia. *Oncogene*. 2017;**36**:4810–6.
22 Chawla AT, Chougoni KK, Joshi PJ, Cororaton AD, Memari P, Stansfield JC et al., CtBP-a targetable dependency for tumor-initiating cell activity and metastasis in pancreatic adenocarcinoma. *Oncogenesis*. 2019;**8**:55.
23 Chen W, Lam SS, Srinath H, Jiang Z, Correia JJ, Schiffer CA et al., Insights into interferon regulatory factor activation from the crystal structure of dimeric IRF5. *Nat Struct Mol Biol*. 2008;**15**:1213–20.
24 Cubillos-Rojas M, Schneider T, Bartrons R, Ventura F, Rosa JL. NEURL4 regulates the transcriptional activity of tumor suppressor protein p53 by modulating its oligomerization. *Oncotarget*. 2017;**8**:61824–36.
25 Balasubramanian P, Zhao LJ, Chinnadurai G. Nicotinamide adenine dinucleotide stimulates oligomerization, interaction with adenovirus E1A and an intrinsic dehydrogenase activity of CtBP. *FEBS Lett*. 2003;**537**:157–60.
26 Thio SS, Bonventre JV, Hsu SI. The CtBP2 co-repressor is regulated by NADH-dependent dimerization and possesses a novel N-terminal repression domain. *Nucleic Acids Res*. 2004;**32**:1836–47.
27 Birts CN, Nijjar SK, Mardle CA, Hoakwie F, Duriez PJ, Blaydes JP et al., A cyclic peptide inhibitor of C-terminal binding protein dimerization links metabolism with mitotic fidelity in breast cancer cells. *Chem Sci*. 2013;**4**:3046–57.
28 Nardini M, Valente C, Ricagno S, Luini A, Corda D, Bolognesi M. CtBP1/BARS Gly172–>Glu mutant structure: impairing NAD(H)-binding and dimerization. *Biochem Biophys Res Commun*. 2009;**381**:70–4.
29 Bi C, Meng F, Yang L, Cheng L, Wang P, Chen M et al., CtBP represses Dpp signaling as a dimer. *Biochem Biophys Res Commun*. 2018;**495**:1980–5.
30 Kreuzer M, Banerjee A, Birts CN, Darley M, Tavassoli A, Ivan M et al., Glycolysis, via NADH-dependent dimerisation of CtBPs, regulates hypoxia-induced expression of CAIX and stem-like breast cancer cell survival. *FEBS Lett*. 2020;**594**:2988–3001.
31 Bellesis AG, Jecrois AM, Hayes JA, Schiffer CA, Royer WE Jr. Assembly of human C-terminal binding protein (CtBP) into tetramers. *J Biol Chem*. 2018;**293**:9101–12.
32 Jecrois AM, Dcona MM, Deng X, Bandyopadhyay D, Grossman SR, Schiffer CA et al., Cryo-EM structure of CtBP2 confirms tetrameric architecture. *Structure*. 2021;**29**:310–9.
33 Madison DL, Wirz JA, Siess D, Lundblad JR. Nicotinamide adenine dinucleotide-induced multimerization of the co-repressor CtBP1 relies on a switching tryptophan. *J Biol Chem*. 2013;**288**:27836–48.
34 Fjeld CC, Birdsong WT, Goodman RH. Differential binding of NAD+ and NADH allows the transcriptional corepressor carboxyl-terminal binding protein to serve as a metabolic sensor. *Proc Natl Acad Sci USA*. 2003;**100**:9202–7.
35 Zhang Q, Piston DW, Goodman RH. Regulation of corepressor function by nuclear NADH. *Science*. 2002;**295**:1895–7.
36 Dcona MM, Damle PK, Zarate-Perez F, Morris BL, Nawaz Z, Dennis MJ et al., Active-site tryptophan, the target of antineoplastic C-terminal binding protein inhibitors, mediates inhibitor disruption of CtBP oligomerization and transcription coregulatory activities. *Mol Pharmacol*. 2019;**96**:99–108.
37 Cambronne XA, Stewart ML, Kim D, Jones-Brunette AM, Morgan RK, Farrens DL et al., Biosensor reveals multiple sources for mitochondrial NAD(+). *Science*. 2016;**352**:1474–7.
38 Canto C, Menzies KJ, Auwerx J. NAD(+) metabolism and the control of energy homeostasis: a balancing act

between mitochondria and the nucleus. *Cell Metab*. 2015;**22**:31–53.
39 Sallin O, Reymond L, Gondrand C, Raith F, Koch B, Johnsson K. Semisynthetic biosensors for mapping cellular concentrations of nicotinamide adenine dinucleotides. *Elife*. 2018;**7**:e32638.
40 Hilbert BJ, Morris BL, Ellis KC, Paulsen JL, Schiffer CA, Grossman SR et al., Structure-guided design of a high affinity inhibitor to human CtBP. *ACS Chem Biol*. 2015;**10**:1118–27.
41 Nichols JC, Schiffer CA, Royer WE Jr. NAD(H) phosphates mediate tetramer assembly of human C-terminal binding protein (CtBP). *J Biol Chem*. 2021;**100351**.
42 Laue TM, Shah B, Ridgeway TM, Pelletier SL. Computer-aided interpretation of analytical sedimentation data for proteins. In: Harding SE, Rowe AJ, Horton JC editors. Analytical ultracentrifugation in biochemistry and polymer science. Cambridge: Royal Society of Chemistry; 1992. p. 90–125.
43 Schuck P. Size-distribution analysis of macromolecules by sedimentation velocity ultracentrifugation and Lamm equation modeling. *Biophys J*. 2000;**78**:1606–19.
44 Stafford WF, Sherwood PJ. Analysis of heterologous interacting systems by sedimentation velocity: curve fitting algorithms for estimation of sedimentation coefficients, equilibrium and kinetic constants. *Biophys Chem*. 2004;**108**:231–43.
45 Cole JL. Analysis of heterogeneous interactions. *Methods Enzymol*. 2004;**384**:212–32.
46 Nardini M, Svergun D, Konarev PV, Spano S, Fasano M, Bracco C et al., The C-terminal domain of the transcriptional corepressor CtBP is intrinsically unstructured. *Protein Sci*. 2006;**15**:1042–50.
47 Blevins MA, Kouznetsova J, Krueger AB, King R, Griner LM, Hu X et al., Small molecule, NSC95397, inhibits the CtBP1-protein partner interaction and CtBP1-mediated transcriptional repression. *J Biomol Screen*. 2015;**20**:663–72.
48 Korwar S, Morris BL, Parikh HI, Coover RA, Doughty TW, Love IM et al., Design, synthesis, and biological evaluation of substrate-competitive inhibitors of C-terminal Binding Protein (CtBP). *Bioorg Med Chem*. 2016;**24**:2707–15.

## Supporting information

Additional supporting information may be found online in the Supporting Information section at the end of the article.

**Fig. S1.** Global SV analysis of the CtBP2 dimer-tetramer equilibrium in the presence of $NAD^+$.